Available online at www.sciencedirect.com
SCIENCE DIRECT®
Thermochimica Acta 415 (2004) 27–34
thermochimica acta
www.elsevier.com/locate/tca

Determination of molar heats of absorption of enantiomers into thin chiral coatings by combined IC calorimetric and microgravimetric (QMB) measurements I. IC calorimetric measurement of heats of absorption

J. Lerchner*, R. Kirchner, J. Seidel, D. Waehlisch, G. Wolf

Institute of Physical Chemistry, TU Bergakademie Freiberg, Leipziger Str. 29, D-09596 Freiberg, Germany

Received 26 May 2003; accepted 8 July 2003

Available online 1 February 2004

Abstract

An IC calorimeter was developed for the investigation of enantioselective gas–surface interactions. The calorimeter is based on a commercially available silicon thermopile chip. Due to its small time constant heat power pulses of 200 μJ are measurable with a deviation of less than 2%. Systematic errors were analyzed by studying the flow rate dependence of the signal. An error level of less than 5% could be estimated by reference measurements with a conventional microcalorimeter. As an example of application the energetics of absorption of the two enantiomers of methyl-2-chloropropionate into a thin film of the chiral receptor octakis(3-*O*-butanoyl-2,6-di-*O*-*n*-pentyl)-γ-cyclodextrin and into an achiral layer of polydimethylsiloxane was studied.

Keywords: Heat conduction calorimetry; Thin film calorimetry; IC calorimeter; Absorption enthalpy; Enantiomers; Chirality

1. Introduction

Chirality is a vital property of nature and of essential importance for the understanding and control of biological processes. Consequently, chiral recognition possesses not only scientific interest but also industrial significance. Especially in the pharmaceutical industry there is a strong move towards enantiomerically pure compounds linked with a growing need for enantioselective separation, preparation and analysis procedures. For the scientific understanding of the mechanism of chiral recognition and separation processes, detailed structural as well as thermodynamic knowledge is required. Thermodynamic data for chiral separation processes, especially enthalpic and entropic contributions to the driving force, have been usually determined by means of temperature dependent chromatographic experiments and applying the van't Hoff analysis [1,2]. However, there are reasonable doubts that these data may be wrong or misleading in some cases due to kinetic problems, change of mechanism in the temperature interval or unfavorable concentrations [3]. Direct calorimetric measurements seem to be more reliable, but small heat effects and heat differences as well as small samples make extremely high demands on the performance of the calorimetric instruments.

Recently, new miniaturized calorimeters were developed especially for the study of gas–surface interactions (e.g. by Smith and Shirazi [4]). The calorimeter described in Ref. [4] has a time constant of approximately 50 s and a heat power resolution of 50 nW. This is sufficient for many applications. However, the reliable measurement of heat pulses less than 10 μJ requires a more rigorous reduction of the time constant of the calorimeter. The use of silicon thermopile chips as heat power detectors can overcome the problem [5,6]. Due to the small thickness of the silicon membrane which contains the thermopile and carries the sample, time constants of less than 50 ms can be achieved. In the first part of this work a refined IC calorimeter based on recently described miniaturized instruments containing commercially available thermopile chips [7] is presented. Spe-

* Corresponding author. Tel.: +49-3731-39-2125; fax: +49-3731-39-3588.
E-mail address: johannes.lerchner@chemie.tu-freiberg.de (J. Lerchner).

0040-6031/$ – see front matter © 2003 Elsevier B.V. All rights reserved.
doi:10.1016/j.tca.2003.07.018

cial emphasis is laid on the analysis of possible systematic errors. It will be demonstrated that calorimeters of this type are suitable for the study of enantioselective gas–surface interactions.

2. Experimental

2.1. Chemicals

The *R*- and *S*-enantiomers of methyl-2-chloropropionate were purchased from Aldrich and used without further purification. Polydimethylsiloxane (PDMS, MoTech) and octakis(3-*O*-butanoyl-2,6-di-*O*-*n*-pentyl)-γ-cyclodextrin (Lipodex E, W.A. König, University of Hamburg) were used as achiral and chiral receptors, respectively. Synthetic air and a certified gas mixture containing 2000 ppm heptane in synthetic air were purchased from Linde Gas AG. For the preparation of homemade gas samples analytical grade heptane from Merck was used.

2.2. The twin-chip calorimetric device

The experimental setup was designed similar to that used in preliminary studies [7]. Two calorimetric chips with integrated thermopiles, XENSOR LCM 2524, coated with a thin film of a gas absorbing receptor are housed in a calorimetric device (Fig. 1), which permits the simultaneous detection of two independent signals generated by the same acting gas. The alternating supply of the sample gas (synthetic air plus acting gas) and the inert reference gas (only synthetic air) is provided by tubes forming a labyrinth path inside a metallic heat exchanger on top of the calorimetric device to ensure a homogeneous temperature. Each detector receives 50% of the total gas flow. The gas flow ends in two elementary nozzles oriented to the center of the chips (Fig. 2). In order to analyze the effects of nozzle orientation two different types of nozzles were constructed: nozzles producing perpendicular (1) and parallel gas streams (2), respectively. In order to improve the temperature stability of the new setup the calorimetric device was mounted in a temperature controlled metal box. The measured temperature fluctuations inside the box during a series of measurements were lower than 10 mK.

A computer controlled gas supply was designed on the basis of three mass flow controllers (MKS) and two compressed gas bottles containing a sample gas stock mixture and synthetic air, respectively. The synthetic air serves as the reference gas as well as for diluting the stock mixture. The desired concentration of the acting gas in the sample was obtained by the appropriate setting of the volume flows. The total volume flow rate used was in the range between 0 and 100 ml min^{-1}. Two valves serves for periodical switching of the two gas flows before entering the calorimetric device. The periodical change between sample gas and reference gas generates a sequence of alternating absorption and desorption effects. For several measurements commercially prepared stock gas mixtures were applied (2000 ppm heptane in synthetic air). Otherwise, the samples were homemade by evaporation of a weighed amount of liquid into a gas bottle and subsequent addition of synthetic air up to a pressure corresponding to the desired normal pressure concentration.

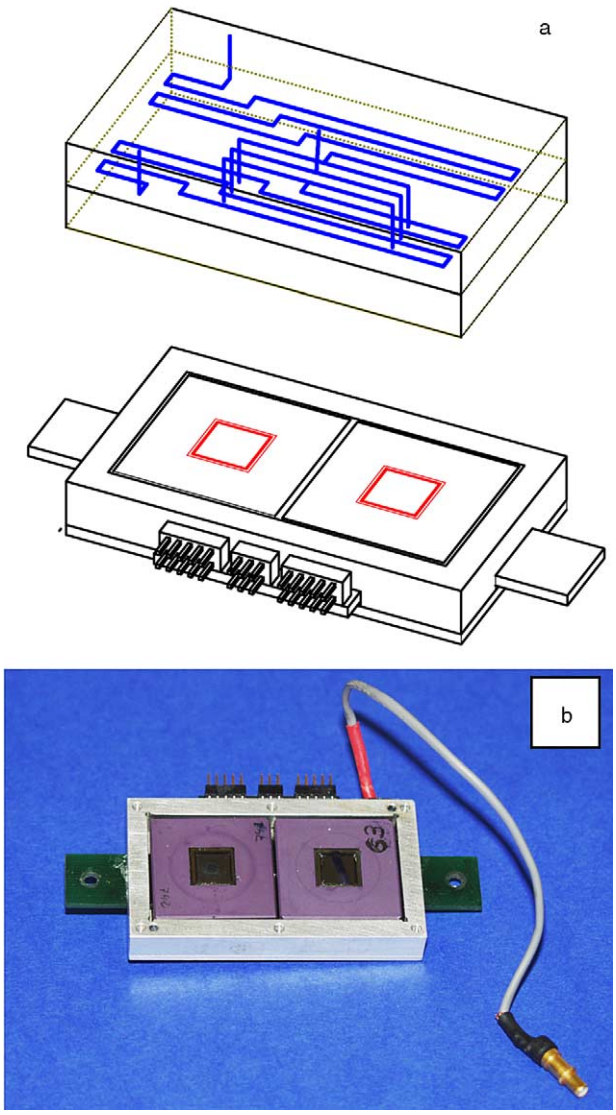

Fig. 1. Scheme (a) and photograph (b) of the calorimetric device. The upper part of (a) comprises the heat exchanger for the inlet gas flows and the nozzles to impinge the gas jets onto the chip surface. The lower part (b) consists of an aluminum frame enclosing the silicon chips and bottom plate.

In order to obtain reproducible absorbing layers on the chip calorimeter with a defined mass, small quantities of the receptor dissolved in dichloromethane were dropped onto the chip surface using a microliter syringe. The receptor mass used in the measurements was $<160\,\mu g$.

Contrary to the previously used experimental setup the actual one was equipped with a KEITHLEY 2700 multimeter based data acquisition system controlled by a computer running a special MATLAB routine. It enables fully automated measuring series around the clock. In parallel to

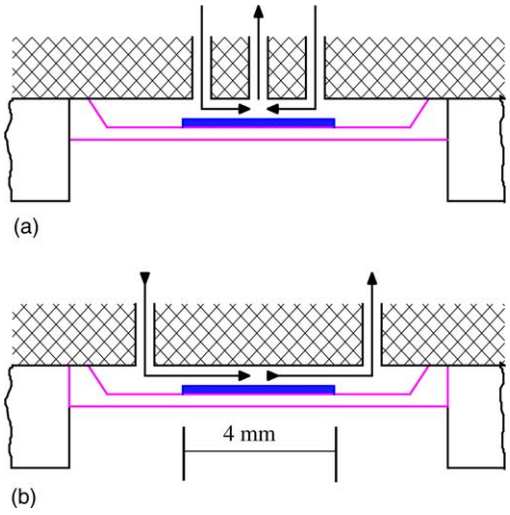

Fig. 2. Gas flow in the nozzles (1) and the nozzles (2).

the thermopile voltage the temperature of the calorimetric device was recorded.

The chip calorimeter was calibrated electrically using the integrated calibration heater of the chips and a separate control unit (power supply and timer).

2.3. Data treatment

Fig. 3 depicts a series of periodic absorption and desorption signal peaks. As previously discussed [8], the shape of the peaks mainly depends on the volume flow rate of the gas, the thickness of the layer, the diffusion coefficient for the distribution of the acting gas within the layer and, as a fixed feature of the device, on the volume of the chamber above the chip membrane. Typically, a half-width of the peaks of 2 s was found. To ensure complete adjustment of the absorption equilibrium, a period time (absorption and desorption) of 120 or 225 s was chosen. Noise reduction is possible by averaging of consecutive signal periods. The averaging was performed off-line after visual inspection of every signal period in order to reject transitory effects and artifacts. From one measuring series usually 20 periods were selected for the averaging procedure. The resulting short term noise of the base line is lower than 0.2 μV corresponding to a temperature resolution of 4 μK, i.e. it is assumed that external temperature perturbations of a few mK will disturb the signals. This can be demonstrated by blank experiments using reference gas instead of sample gas. In Fig. 4a the averaged periodic signal of a blank experiment is shown. Base line shift and transient effects around the valve switching points are mainly caused by incomplete temperature adjustment of the gas. This has been proved in separate experiments with heated input gas flows (not shown here). On the other hand, the temperature induced distortions are changing slowly. Thus, the correction of blank effects is possible by subtraction of the averaged signals from absorption and blank measurements. Fig. 4b demonstrates that the subtraction of two consecutive, averaged blank signals almost provides complete compensation of the temperature caused distortions. In Fig. 4c a corrected absorption–desorption signal is reported showing a perfect base line. Numerical integration of the peaks provides the integral heats of absorption and desorption, respectively. An algorithm analyzing the slope of the base line was applied to find an appropriate range of integration.

The signals from the Joule heating measurements were processed in the same way as the absorption ones. Fig. 5 depicts an example for an averaged signal period generated by periodical Joule heating. The voltage difference at steady states provides the calibration information. The cor-

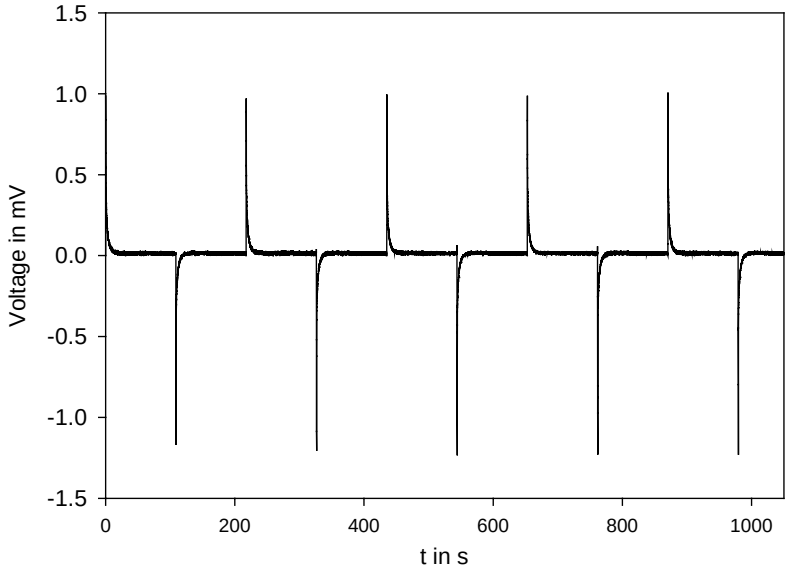

Fig. 3. Part of a series of periodic absorption and desorption signal peaks ($v = 60\,\mathrm{ml\,min^{-1}}$, $c_{hep} = 1000\,\mathrm{ppm}$, 100 μg PDMS, $T = 225\,\mathrm{s}$).

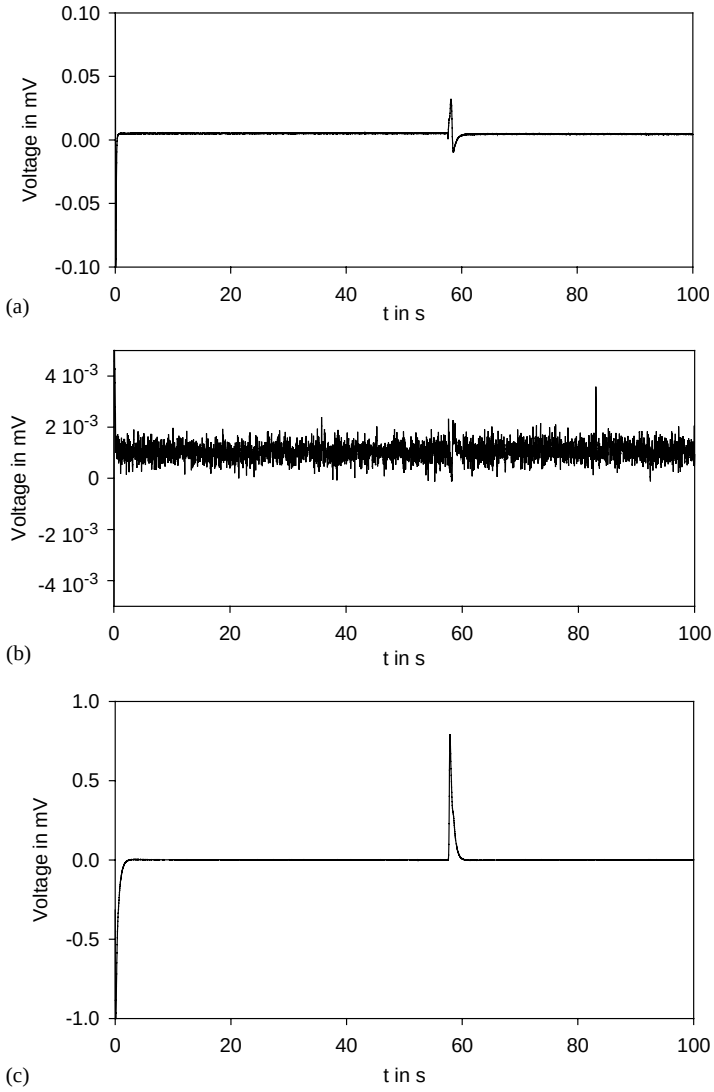

Fig. 4. Blank corrections of the absorption–desorption signals: (a) averaged period of a blank measurement; (b) effect of subtraction of two consecutive averaged blank periods; (c) blank corrected absorption–desorption signal period ($v = 60\,\mathrm{ml\,min^{-1}}$, $c_{\mathrm{hep}} = 2000\,\mathrm{ppm}$, 85 μg PDMS, $T = 120\,\mathrm{s}$).

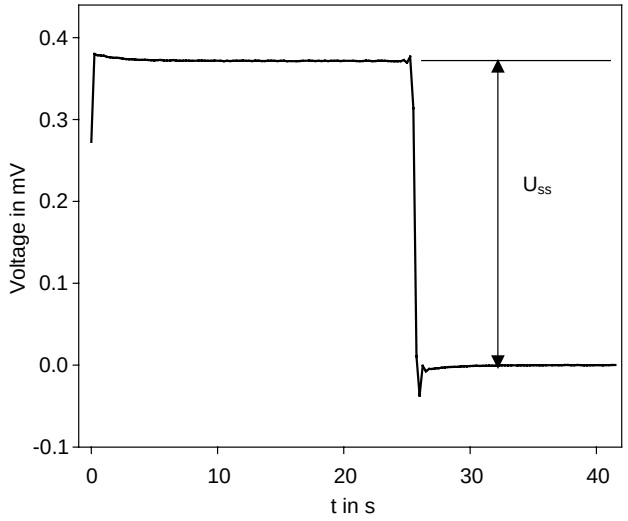

Fig. 5. Averaged period of a Joule heating signal period ($p_{\mathrm{el}} = 170\,\mu\mathrm{W}$).

responding heat power generated electrically was measured off-line.

2.4. Reference measurements with a conventional microcalorimeter

Reference absorption measurements were carried out by means of a conventional twin heat conduction calorimeter (TAM 2277, Thermometric, AB Sweden). The 4 ml high performance calorimeter equipped with the RH-perfusion unit and a 1 ml stainless steel cell was used for the experiments. The measurements were performed using a sample gas mixture of 1000 ppm heptane in synthetic air, a constant total flow rate of $1.6\,\mathrm{ml\,min^{-1}}$ and a temperature of 25 °C. Two mass flow controllers (BRONKHORST) were used for sample gas and synthetic air, respectively, each connected to a three-way magnetic valve to switch periodically between the sample gas (sorption) and synthetic air (desorption). In order

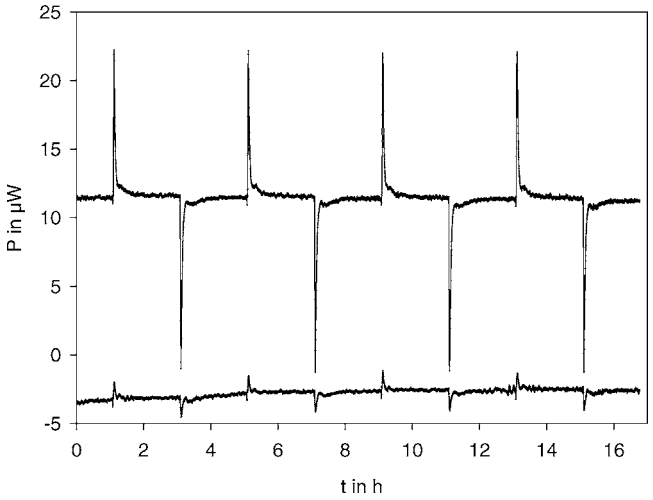

Fig. 6. Part of series of periodic sorption, desorption and blank signal peaks ($v = 1.6\,\mathrm{ml\,min^{-1}}$, $c_{hep} = 1000\,\mathrm{ppm}$, 1 mg PDMS, TAM calorimeter).

to prepare a nearly homogeneous thin film of PDMS inside the calorimetric cell, a known volume of a PDMS solution in dichloromethane was filled in and the solvent was evaporated under permanent rotation of the cell. A sorption (desorption) step was always started after reaching chemical and thermal equilibrium in the calorimeter. The heat flow was recorded as a function of time and converted into enthalpies by integration of the appropriate peaks. Blank effects were corrected by subtracting the results of blank experiments with synthetic air at identical experimental conditions (Fig. 6).

The TAM microcalorimeter was calibrated electrically applying the standard procedure described in the user manual at a constant total flow of $1.6\,\mathrm{ml\,min^{-1}}$ synthetic air.

3. Results and discussion

3.1. Calorimetric monitoring of the absorption process

In order to check whether the measured effects are really caused by the absorption–desorption process, the absorption of heptane by a polymer layer (PDMS) was investigated. In the range up to 2000 ppm of heptane Henry's law should be fulfilled [9], i.e. the amount of absorbed gas should change linearly with its concentration in the sample gas. Consequently, a linear relationship between the measured heat and the concentration should be expected for the absorption as well as for the desorption. Furthermore, heats of absorption and desorption have to be identical at the same experimental conditions. The results shown in Fig. 7 confirm both facts, i.e. the measured heats can be assigned to the absorption–desorption process.

3.2. Analysis of the convective heat loss

The heat power calibration of the device can be performed by Joule heating using the integrated chip-heater. Systematic errors of this procedure could be caused by lateral sensitivity changes in the silicon membrane and by convective heat loss. If the receptor layer is located inside the most sensitive area of the chip (the area which is surrounded by the hot junctions of the thermopile), the sensitivity dependence on the shape of the layer is negligible with an error of less than 1% related to the Joule heating sensitivity [10]. This can be described by a *shape factor* as proposed by Torra et al. [11]. Besides some preliminary experiments [5], the influence of the convective heat loss on the accuracy of the measured heats of absorption in a flow-through chip calorimeter was not studied systematically up to now.

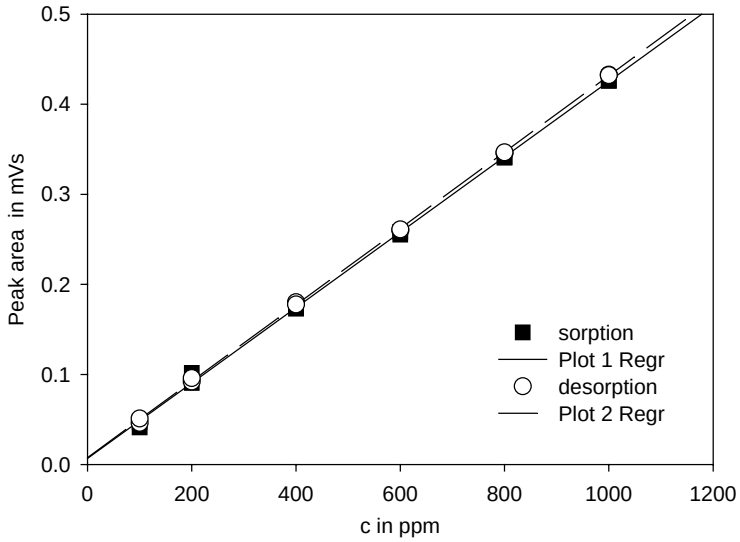

Fig. 7. Plot of the peak areas of absorption and desorption against the concentration of heptane (85 µg DMPS, $v = 60\,\mathrm{ml\,min^{-1}}$).

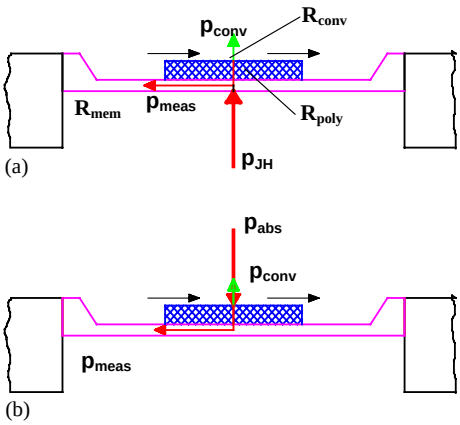

Fig. 8. Heat flows and thermal resistances in the chip-layer system: (a) Joule heating; (b) absorption. p_{JH}, input power of Joule heating; p_{abs}, input power of absorption; p_{conv}, convective heat loss; p_{meas}, measured heat power; R_{mem}, thermal resistance of the silicon membrane; R_{poly}, thermal resistance of the absorbing layer; R_{conv}, thermal resistance of convective heat exchange.

The convective heat loss, i.e. the heat which is transferred between the chip surface and the gas stream, depends on the surface area, the temperature difference between surface and gas and the average convection coefficient. The latter depends on the volume flow rate, the geometry of the fluid stream and some properties of the gas. A quantitative description of the convective heat loss is possible by characteristic dimensionless numbers [12].

A discussion of systematic errors caused by forced convection requires the examination whether a Joule heating signal is reduced by convective heat loss similar to a signal generated by a gas–receptor interaction. The thermal resistance of the receptor layer is the crucial parameter as explained by the simple scheme in Fig. 8. According to Fig. 8, concentrated thermal resistances are assumed for describing the heat transfer inside the chip membrane and through the absorbing layer as well as for the convective heat loss. Thus, by applying Kirchhoff's laws, relations between the convective heat loss p_{conv} and the measured heat power p_{meas} can be derived for Joule heating and gas–surface interaction, respectively. The measured heat power is that part of the total heat power which is converted into the measured voltage signal by the thermopile. Eq. (1) indicates that the influence of the receptor layer differs from Joule heating (1a) to absorption (1b). Increasing the thermal resistance of the absorbing layer, e.g. due to increasing the thickness, should decrease the conductive heat loss during Joule heating. For the absorption an opposite effect should be expected. Therefore, it is important to compare the volume flow rate dependence of Joule heating and absorption signals:

$$\frac{p_{conv}}{p_{meas}} = \frac{R_{mem}}{R_{conv}} \left(\frac{1}{1 + R_{poly}/R_{conv}} \right) \quad (1)$$

$$\frac{p_{conv}}{p_{meas}} = \frac{R_{mem}}{R_{conv}} \left(1 + \frac{R_{poly}}{R_{mem}} \right) \quad (2)$$

Table 1
Normalized linear slopes of the signal change with respect to the volume flow rate for nozzle 1

Layer	Normalized slope (ml min^{-1}) (Joule heating)	Normalized slope (ml min^{-1}) (absorption)
L0	-5.92×10^{-4}	
L1	-5.89×10^{-4}	-5.04×10^{-4}
L2	-5.97×10^{-4}	-4.89×10^{-4}

L0, L1, L2 symbolize the different polymer layers (L0, empty; L1, 20 μg PDMS; L2, 45 μg PDMS).

In Fig. 9 the volume flow rate dependencies of both the steady-state voltage from Joule heating experiments and the heptane absorption peak areas are shown for nozzles 1 and 2. In the case of nozzle 1, the dependencies were examined for two different amounts of PDMS on the chip. The flow conditions caused by nozzle 1 lead to a significant volume flow rate dependence of the signals. In Table 1 the data of normalized slopes are summarized. Normalized slopes were calculated by dividing the slope of the linear part of the curve by the zero flow rate value in the case of Joule heating or by the extrapolated one in the case of heptane absorption, respectively. It is demonstrated that the relative change of the parameters with respect to the flow rate is quite similar for Joule heating and heptane absorption. Furthermore, no significant influence of the polymer layer on the flow rate dependence could be detected. The situation improves drastically if nozzle 2 is applied. In this case, the volume flow rate dependence is reduced by a factor of 5 as shown for the Joule heating signals. Because of the larger scatter of the absorption data no significant effect of the volume flow rate can be observed. Because of optimal peak integration in all experiments a fixed volume flow rate of 60 ml min^{-1} was chosen.

In summary, one can conclude that systematic errors due to convective heat loss effects should be smaller than 2% if the integrated heater is applied for calibration.

3.3. Comparison between IC calorimeter and TAM

Because of the lack of a certified test reaction for solid–gas interactions comparative sorption experiments were carried out with the IC and the TAM calorimeter in order to verify the expected accuracy of the IC calorimetric measurements. Heats of sorption were measured in dependence of the mass of PDMS. In the case of the IC calorimeter the mass of PDMS varied from 75 to 160 μg and for the TAM calorimeter from 650 to 1200 μg. In both cases the same heptane sample mixture was used. For both calorimeters a linear dependence of the heat of absorption from the mass of PDMS was obtained. From the slopes the following sorption enthalpies were calculated: TAM calorimeter 1.71 ± 0.17 J/g, IC calorimeter 1.86 ± 0.08 J/g (based on the electrical calibration). Considering the experimental uncertainties, the difference of the two results is not significant. The relative large error of the TAM results is due to an unfavorable

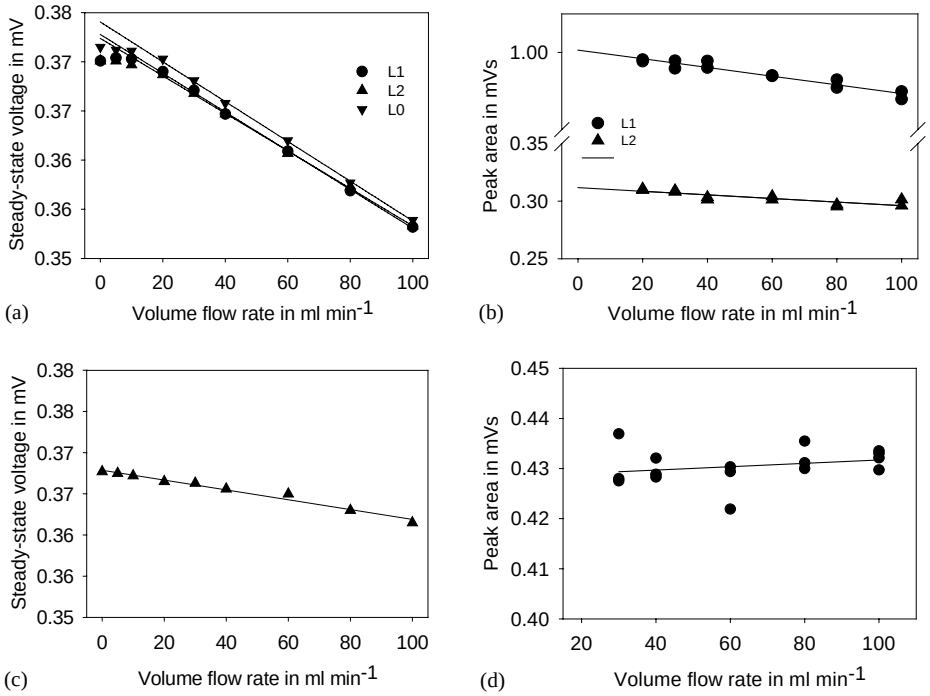

Fig. 9. Volume flow rate dependence of the signal parameters: (a) steady-state voltage data from Joule heating, nozzle 1; (b) peak areas of absorption, nozzle 1; (c) steady-state voltage from Joule heating, nozzle 2; (d) peak area of absorption, nozzle 2. L0, L1, L2 symbolize the different polymer layers (L0, empty; L1, 20 μg PDMS; L2, 45 μg PDMS).

signal-to-noise ratio caused by relatively long equilibration times and small signals. This result also illustrates the advantage of the small time constant of the IC calorimeter for thin film sorption studies. In summary, this comparative experiment confirmed the reliability of the electrical calibration of the IC calorimeter at the applied experimental conditions.

3.4. Determination of heats of absorption of enantiomers into chiral receptors

The refined and optimized IC calorimeter was applied to investigate the energetics of absorption of the two enantiomers of methyl-2-chloropropionate into a thin film of the chiral receptor Lipodex E and into an achiral layer of

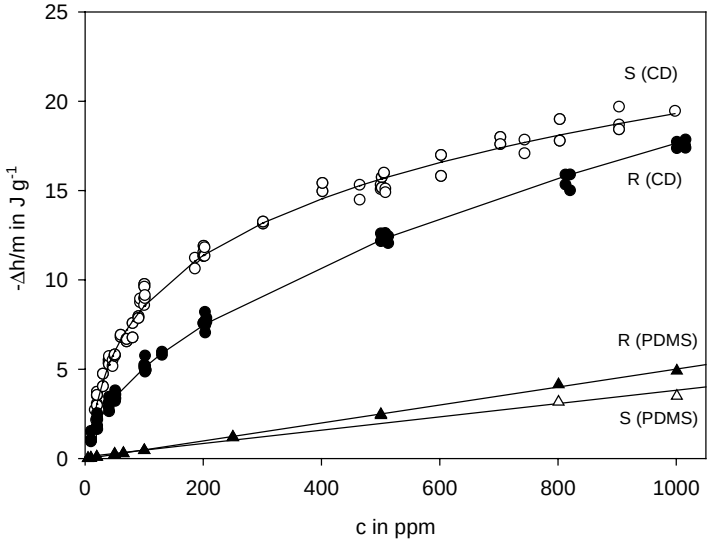

Fig. 10. Heats of absorption of the two enantiomers of methyl-2-chloropropionate into the chiral receptor (2.5 μg Lipodex E, $v = 60\,\mathrm{ml\,min^{-1}}$) and into the achiral receptor (100 μg PDMS, $v = 60\,\mathrm{ml\,min^{-1}}$).

PDMS. Results obtained with receptor layers of 2.5 μg (Lipodex E) and 100 μg (PDMS) are shown in Fig. 10. The results demonstrate that the IC calorimeter is capable of measuring small heats of absorption in thin films with high sensitivity and precision. The non-linear dependence of the heats of absorption into the cyclodextrin on the enantiomer concentration and the comparatively large heat effects indicate specific enantiomer–receptor interactions. The preferred interaction of the *S*-enantiomer, also known from chromatographic separation experiments [13], is expressed by considerable larger heat effects, especially at low enantiomer concentrations. In contrast to the cyclodextrin receptor, the heats of absorption into PDMS show a linear dependence on the enantiomer concentration, the effects are much smaller and the difference between the enantiomers is small. This result is typical for a non-specific interaction which could be expected for an achiral receptor.

A detailed thermodynamical analysis of the calorimetric results together with microgravimetric (quartz microbalance) results, including modeling of the absorption isotherms, calculation of thermodynamic absorption data (ΔG, ΔH, ΔS) and discussion of chiral discrimination thermodynamics, will be presented in the forthcoming second part of this paper.

4. Conclusions

The measurement of heats of absorption of gas into thin films is one of the fields of application where IC calorimeters are unrivaled. Due to the fast mass transfer inside thin films the advantage of the small time constants of IC calorimeters takes effect. Even advanced conventional microcalorimeters (like the TAM 2277) with a heat power resolution in the nW range do not permit satisfactory precision for measuring short heat pulses of a few μJ. Despite of the open structure of IC calorimeters systematic errors are less than 5% with respect to Joule heating calibration. Therefore, IC calorimetry should be the method of choice if sophisticated energetic studies of interactions with thin films are intended.

Acknowledgements

The authors thank the German Research Council (Deutsche Forschungsgemeinschaft) for financial support (WO 576/11-1). The cooperation of the groups in Freiberg and Barcelona was supported by integrated HA 1999-0087 (MCT, Spain) and 314-Al-e-dr (DAAD). Furthermore, the authors would like to thank W.A. König (University of Hamburg) for some inspiration to do this work and for donating the cyclodextrin sample.

References

[1] I. Hardt, W.A. König, J. Microcol. Sep. 5 (1993) 35.
[2] V. Schurig, M. Juza, J. Chromatogr. A 757 (1997) 119–135.
[3] H. Naghibi, A. Tamura, J.M. Sturtevant, Proc. Natl. Acad. Sci. U.S.A. 92 (1995) 5597.
[4] A.L. Smith, H.M. Shirazi, J. Therm. Anal. Calc. 59 (2000) 171.
[5] J. Lerchner, A. Wolf, G. Wolf, J. Therm. Anal. Calc. 57 (1999) 241.
[6] J. Lerchner, A. Wolf, A. Weber, R. Hüttl, G. Wolf, in: W. Ehrfeld (Ed.), Microreaction Technology, Industrial Prospects', Springer, Berlin, Heidelberg, 2000, p. 469.
[7] D. Caspary, M. Schröpfer, J. Lerchner, G. Wolf, Thermochim. Acta 337 (1999) 19.
[8] J. Lerchner, D. Caspary, G. Wolf, Sens. Actuators B 70 (2000) 57.
[9] K.D. Schierbaum, A. Gerlach, M. Haug, W. Göpel, Sens. Actuators A 31 (1992) 130.
[10] J. Lerchner, G. Wolf, C. Auguet, V. Torra, Thermochim. Acta 382 (2002) 65.
[11] V. Torra, C. Auguet, J. Lerchner, P. Marinelli, H. Tachoire, J. Therm. Anal. Calc. 66 (2001) 255.
[12] F.P. Incropera, D.P. DeWitt, Introduction to Heat Transfer, Wiley, New York, 2002.
[13] K. Bodenhöfer, A. Hierlemann, M. Juza, V. Schurig, W. Göpel, Anal. Chem. 69 (1997) 4017.